Berkala **PENELITIAN HAYATI**

ISSN: 08526834 | E-ISSN:2337-389X

Volume 27| No. 1| December | 2021

Original Article

Prediction of protein venom epitope (kistomin) from *Calloselasma rhodostoma* using immunoinformatics to design vaccine based on epitope

Zyana Fithri Nur Faizah[1,2,3], Nia Kurniawan[1,3], Fatchiyah Fatchiyah[1,2*]

[1]Department of Biology, Faculty of Mathematics and Natural Science, Universitas Brawijaya, Malang, Indonesia

[2]Research Center of Smart Molecule of Natural Genetics Resources (SMONAGENES), Universitas Brawijaya, Malang, Indonesia

[3]NK Research, Faculty of Mathematics and Natural Science, Universitas Brawijaya, Malang, Indonesia

Abstract

Vaccines based on epitope are alternative treatments for snakebite aside from anti-venom immunoglobulin, which is specific and not cross-reaction. However, the potential kistomin epitope has not been known. This study identified the region of T cells epitope and evaluated their immunogenicity to induce an immune response by *in-silico*. Sequences of kistomin were collected from Swiss-Prot with ID P0CB14. The physico-chemical and conserved domain of kistomin were predicted by using ProtParam and the NCBI database. The T cell epitope was predicted by using the Artificial Neural Network (ANN) method on the IEDB website. Epitopes with MHC-IC50 values >250 nM were further analyzed for conservation and immunogenicity on the IEDB website as well. After that, the candidate 9-mer epitope was interacted by simulated docking with four Major Histocompatibility Complex (MHC) molecules (5ENW, 6VB0, 3PGD, 6DIG). The conserved 9-mer epitope candidates with high immunogenicity and having similarities with the 15-mer epitope candidates are 4-VLLVTICLA-12 and 27-NVNDYEVVY-35. The 4-VLLVTICLA-12 candidate epitope interacted at β-sheet structure of four MHC. In contrast, The 27-NVNDYEVVY-35 candidate epitope interacted at α-helix and β-sheet structures of HLA-B*15:02 MHC. This study suggested 27-NVNDYEVVY-35 is potentially used as vaccine from envenomation *Calloselasma rhodhostoma*. In future studies, other alelles can be used to predict epitope from metalloproteinase domain in kistomin.

Keywords: Epitope, kistomin, MHC, vaccine

Received: July 12, 2021 Revised: September 15, 2021 Accepted: September 15, 2021

Introduction

Cases of envenomation in Indonesia were estimated to be >100,000 cases annually with a mortality rate of 101-1000 people per year (Kasturiratne et al., 2008). One of the envenomation was caused by *Calloselasma rhodostoma*. *C. rhodostoma* is classified in the category of high medical importance and is spread in Southeast Asia and in Indonesia spread over on Java, Karimun, and Kangean (Tang et al., 2019; Das, 2010).

C. rhodostoma snake venom from various geographical locations is dominated by kistomin (Tang et al., 2019). Kistomin belongs to the Snake Venom Metalloproteinase (SVMP) group whose it has hemorrhagic activity (Tang et al., 2016). Kistomin is included in P-I subfamily of SVMPs. Kistomin have metalloproteinase domains, pro-domains and signal sequences. Metalloproteinase enzymes are active when the peptide signal and pro-domain sequences were released (Olaoba et al., 2020). The SVMP activation causes Extracellular Matrix (ECM) degradation and eliminate cell viability (Gutiérrez et al., 2016)

ECM degradation and cell viability cannot stop if SVMP are not neutralized or inactivated. The technology has been developed that is anti-venom immunoglobulin. Anti-venom immunoglobulin works specifically and causes cross reaction (León et al., 2011). Indonesia has been developed anti-venoms immunoglobulin which is SABU (Serum Bisa Ular) (WHO, 2010). SABU can neutralize protein venom from *Calloselasma rhodostoma*. SABU contains albumin which it can induces hypersensitivity in respiratory disorders and shock due to anaphylactoid. The cost of purified albumin production by maximum purification is significantly high. In addition, giving antivenom should be done every time if get bitten by a snake (Bermúdez-Méndez et al., 2018).

One of the innovation strategy to treat envenomation was the immunization vaccine methods. Epitope-based vaccine has several advantages, including specific response, no unwanted immune response, an adjustable composition and easier production (Khan et al., 2015; Li et al., 2014; Parvizpour et al., 2020; Sette & Fikes, 2003). It can increase efficacy, safety, and affordability, and treatment is only done once to induce immunity (Bermúdez-Méndez et al., 2018).

Epitope-based vaccine production has three important steps, including epitope mapping, immunogen construction, and evaluation of vaccine effectiveness. Recently, computational epitope mapping methods have been used to reduce time, cost and failure (Parvizpour et al., 2020). The mapping has several stages to evaluate immunogenicity, evaluate epitope conservation, and eliminate epitope which to have side effects. These stages can be solved by using the immunoinformatics method (Bui et al., 2007; León et al., 2011). Immunoinformatics was used to mapping epitope for PLA_2 from *Bungarus candidus* and *Bungarus caerules* (Kurniawan & Kurniasari, 2020; Muhammad Ashraf et al., 2014). Epitope-based vaccine for kistomin hasn't yet researched. Therefore, this study aimed to identify the epitope region of kistomin (the venom of *Calloselasma*

* Corresponding Author:
Fatchiyah Fatchiyah
Research Center of Smart Molecule of Natural Genetics Resources (SMONAGENES), Universitas Brawijaya, Indonesia
Phone: +62 341 554401 Fax: +62 341 554403
E-mail: fatchiya@ub.ac.id

http://dx.doi.org/10.23869/bphjbr.27.1.20213
Published by © PBI East Java. Open Access www.berkalahayati.org

rhodostoma) and evaluate its immunogenicity in inducing an immune response by *in-silico*.

Methods

Protein sequence retrieval

The sequence of kistomin from *Calloselasma rhodostoma* was retrieved from the Uniprot database (http://www.uniprot.org). The accession number of the protein kistomin sequence is P0CB14.

Secondary structure prediction

The physico-chemical properties of the secondary structure of kistomin were predicted by the ProtParam tool on the ExPASy website server (https://web.expasy.org/protparam). This ProtParam tool was used to predict the location of negative and positive residues, formulas, exclusion coefficients and instability indexes, aliphatic indexes and Grand Average of Hydropathicity (GRAVY)

Identification of the conserved domain

The identification of the conserved domain was carried out by alignment of the kistomin sequences with members of the protein superfamily Cd00206 and pfam0087. Identification was carried out with the NCBI database (https://www.ncbi.nlm.nih.gov/Structure/cdd/wrpsb.cgi).

Prediction of T cell receptor epitopes (MHC-I and MHC-II)

T cell epitopes were predicted from the kistomin sequence by using the Immune Epitope and Analysis Database (IEDB). The prediction is based on the binding interaction between the epitope with MHC class I (MHC-I) and MHC class II (MHC-II). Epitope and MHC-I interactions were predicted by using the MHC-I Processing Prediction tool at IEDB (http://tools.iedb.org/mhci/tcell) by using the Artificial Neuronal Network (ANN 4.0) prediction method (Andreatta & Nielsen, 2016; Lundegaard et al., 2008; Nielsen et al., 2003). The alleles used for prediction were 51 alleles with the length of the epitope determined as long as 9 amino acids, then were screened virtually by MHC-II binding using MHC-II binding prediction tool (https: /tools.iedb.org/mhcii) with the Artificial Neutral Network (NN-align 2.3) prediction method. The epitopes vaccine were predicted from 27 alleles and determined the length of the epitope was 15 amino acids. Then, the predicted results of the MHC-I epitope were selected based on the IC50 less than 250 nM and MHC-II epitope were selected based on the IC50 less than 200 nM and R value less than 10% (Kurniawan & Kurniasari, 2020).

Epitope conservancy and immunogenicity analysis

Kistomin epitope concervancy was analyzed by using the tools available at IEDB (https://tools.iedb.org/concervancy/). Kistomin sequence was compared with 22 proteins which it were had similarity, had complete sequences and was reviewed by UNIPROT (Table S1). Furthermore, the selection of peptide sequences with conservation values above 50% were carried out for immunogenicity analysis. Immunogenicity analysis was carried out using the tools available in the IEDB (https://tools.iedb.org/immunogenicity/).

Docking simulation

The immunogenicity of Kistomin Epitope was evaluated by docking simulation. The docking simulation was carried out by interacting the potential candidate epitope with two molecules of MHC-I allele HLA-A*0201 (PDB ID: 5ENW) and allele HLA-B*1502 (PDB ID: 6VB0) and two molecules of MHC-II allele HLA DRA1/DRB1 (PDB). ID: 3PGD) and allele HLA-DQA1*01:02/DQB1*06:01 (PDB ID: 6DIG). The epitope candidate was modeled with HHpred (https://toolkit.tuebingen.mpg.de/tools/hhpred) to obtain a three-dimensional structure. The MHC molecular structure was prepared by removing water molecules and ligand molecules using the Discovery Studio Visualizer V16.1.0.15350 software. Docking simulation was done with Hex 8.0 software, with the correlation type shape + electro and other parameters as default (Ahkam et al., 2020; Tapiory et al., 2020) Molecular docking results were analyzed using Discovery Studio Visualizer V16.1.0.15350 and Ligplot V.1.4.5 (Fatchiyah et al., 2015; Kurniawan & Kurniasari, 2020). The interaction between the Toxoplasma epitope "GLKEGIPAL" and the MHC-I molecule HLA-A*0201 allele was used as a comparison.

Results

Analysis of physico-chemical properties and identification of conserved domains of kistomin

The kistomin sequence consists of 417 amino acids. Molecular weight of kistomin was predicted 47445.99 Da. Kistomin was stable protein with stability index more than 40. Kistomin have residues with positive charge. Kistomin was a hydrophilic protein with a GRAVY value and an isoelectric point (pI) of 5.91 (Table 1). Kistomin performed conserved domain in residues number 32 – 152 and 200 – 385.

Table 1. Physico-chemical properties of kistomin protein from *C. rhodostoma*

Criteria	Assesment
Number of amino acids	417
Molecular weight	47445.99
Isoelectric pH	5.91
No. of negatively charged residues (Asp + Glu)	58
No. of positively charged residues (Arg + Lys)	49
Formula	$C_{2105}H_{3264}N_{558}O_{639}S_{26}$
Extinction coefficient	46300 47050
Instability index	37.21
Aliphatic index	71.75
Grand average of hydropathicity (GRAVY)	-0.518

Prediction of T cell epitope (predicted MHC-I & MHC-II binding)

There 74 of 362 epitopes can bind strongly with some alleles from HLA-A to HLA-C. Certain alleles of MHC-II recognized with 156 of the 319 epitopes predicted by strong binding. (Table S2 and S3). In addition, 62 of 74 epitopes were recognized with MHC-I and MHC-II allele. (Table S4). The epitope was recognized to MHC-II consists of 15 amino acids and 9 core-peptides (Table S3).

Epitope conservation and immunogenicity analysis

From 74 epitopes, only five epitopes was have a conservation value more than 50%. In addition, from the five conserved epitopes, only 3 epitopes have high immunogenicity with positive immunogenicity values. The 9-mer epitope is high conservation and immunogenicity, only interacted with one MHC-I allele (Table 2). The conserved peptide has high immunogenicity in the signal peptide domain (4-VLLVTICLA-12) and pro-peptide domain (27-NVNDYEVVY-35), both of them were not in the conserved domain.

Similarity of candidate MHC-I molecular epitope and candidate MHC-II

The 9-mer epitope interacted with the MHC-I molecule and the 15-mer epitope bound to the MHC-II molecule with the 9-mer core peptide. The 9-mer epitope has high immunogenicity also has similarity with the 15-mer epitope except the 23-LESGNVNDY-31. Epitope 27-NVNDYEVVY-35 similar with four candidate epitopes. It was recognized by several alelles from HLA-DRB1. Furthermore, 4-VLLVTICLA-12 has similar epitope which it recognized with several alelles HLA DQA1/DQB1 and DPA1/DPB1 (Table 2).

Table 2. Conservation values immunogenicity and interactions of 9-mer and 15-mer peptides that interacted with MHC-I and MHC-II molecules of several alleles

Peptide (9-mer)	Alel	Conservancy	Immunogenicity	Peptida (15-mer)	Alel
27-NVNDYEVVY-35	HLA-B*15:02	5455%	0.16983	25-SGNVNDYEVVYPRKI-39	HLA-DRB1*07:01
				26-GNVNDYEVVYPRKIT-40	HLA-DRB1*07:01
					HLA-DRB1*09:01
				27-NVNDYEVVYPRKITA-41	HLA-DRB1*07:01
					HLA-DRB1*09:01
					HLA-DQA1*05:01/DQB1*04:02
				26-GNVNDYEVVYPRKIT-40	HLA-DRB1*09:01
4-VLLVTICLA-12	HLA-A*02:01	7727%	0.14904	1-MIEVLLVTICLAAFP-15	HLA-DQA1*01:02/DQB1*05:01
					HLA-DQA1*02:01/DQB1*03:01
				3-EVLLVTICLAAFPYQ-17	HLA-DQA1*01:02/DQB1*05:01
					HLA-DQA1*02:01/DQB1*03:01
					HLA-DPA1*01:03/DPB1*02:01
				4-VLLVTICLAAFPYQG-18	HLA-DQA1*01:02/DQB1*05:01
				2-IEVLLVTICLAAFPY-16	HLA-DQA1*02:01/DQB1*03:01
					HLA-DPA1*01:03/DPB1*02:01
23-LESGNVNDY-31	HLA-B*18:01	6364%	0.02046	-	-

Docking simulation

The 27- NVNDYEVVY-35 epitope interacted with the α-helix and β-sheet region structure in domain A of the MHC-I HLA-A*02:01 while the epitope interacted with the HLA-B*15:02 in the α-helix region, even though the end of the peptide still like interacted with the α-helix structure. Futhermore, the 4-VLLVTICLA-12 epitope interacted at the β-sheet region of the HLA-A*02:01 and HLA-B*15:02. The two epitopes interacted with the HLA-A*02:01 and HLA-B*15:02 at different residues. The hydrogen bond was produced by the interaction of the 27-NVNDYEVVY-35 epitope was less than the 4-VLLVTICLA-12 (Figure 1). In addition, there were several other bonds, like hydrophobic, electrostatic, and other bonds between the epitope and the two MHC-I molecules. The 4-VLLVTICLA-12 epitope provided an atomic donor for the Asp30 residue in both MHC-I molecules. The "GLKEGIPAL" epitope also donated its

atom to the Asp30 residue in the HLA-A*02:01. The binding energy of 4-VLLVTICLA-12 with HLA-B*15:02 was lower than 4-VLLVTICLA-12 with HLA-A*02:01. Meanwhile, the binding energy 27-NVNDYEVVY-35 with HLA-B*15:02 was lower than binding energy 27-NVNDYEVVY-35 with HLA-A*02:01 (Table 3).

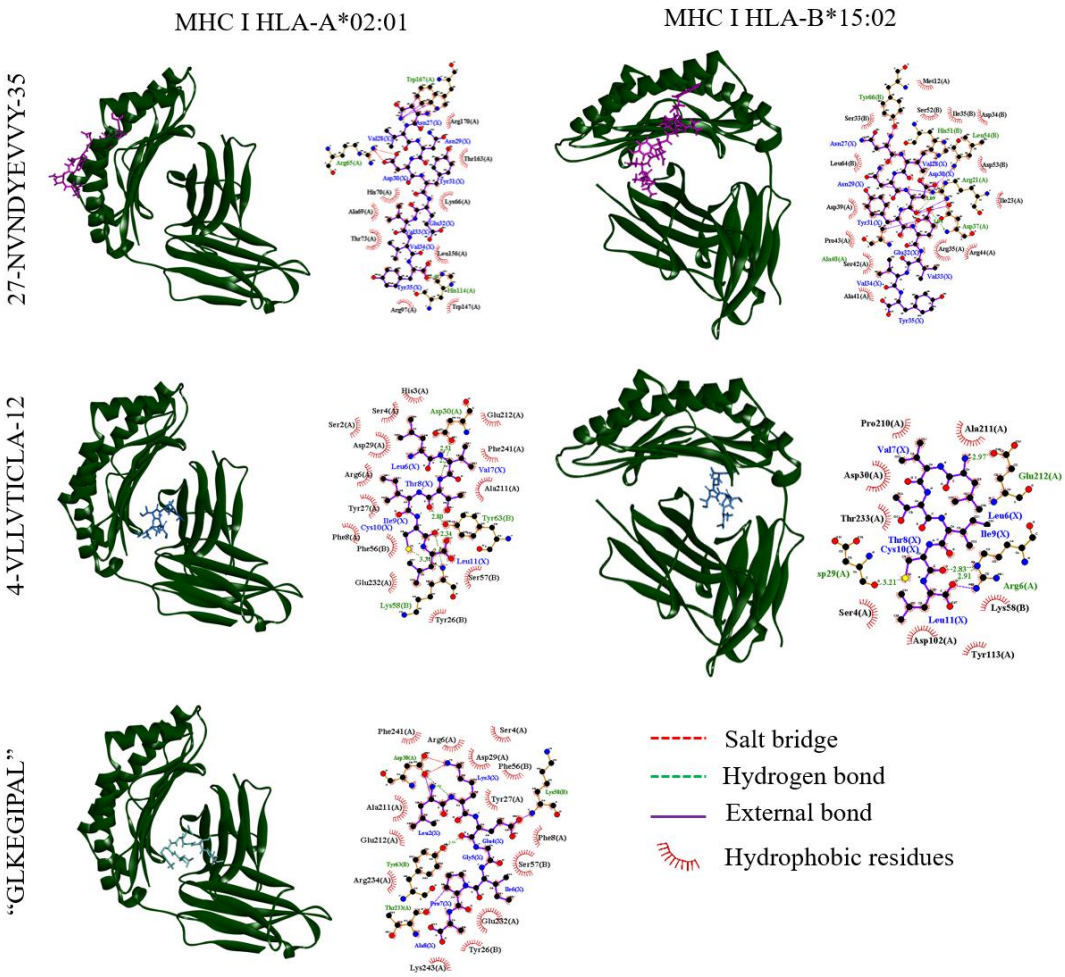

Figure 1. Interaction of 4-VLLVTICLA-12 dan 27-NVNDYEVVY epitope with MHC-I HLA-A *02:01 dan HLA-B*15:02. The color in 3D view denote as HLA (Green) 27-NVNDYEVVY epitope (Purple) 4-VLLVTICLA-12 epitope (dark blue) and "GLKEGIPAL" epitope (blue).

The 27-NVNDYEVVY-35 and 4-VLLVTICLA-12 epitopes interacted with MHC HLA DRA1/DRB1 at β-sheets structure of the molecule. The 27-NVNDYEVVY-35 epitope also interacted with the HLA-DQAI*01:02/DQBI*06:01 in the α-helix structure although most of it interacted with β-sheet structure. Meanwhile, 4-VLLVTICLA-12 interacted only in β-sheet structure of HLA DQAI*01:02/DQBI*06:01. Distance of the hydrogen bond between 27-NVNDYEVVY-35 epitope residue and the residue of DRA1/DRB1 was farther than the 27-NVNDYEVVY-35 epitope residue with the residue of HLA-DQA1*01:02/DQB1*06:01. The Cys10 residue on the 4-VLLVTICLA-12 epitope plays a role in forming hydrogen bonds in the two MHC-II molecules. The Cys10 residue interacted by hydrogen bond with Ala52 residue in domain A of HLA DRA1/DRB1 molecule with a distance of 3.14 Å and interacted with Arg149 in domain B of the HLA-DQA1*01:02/DQB1*06:01 molecule with a distance of 2.7 Å (Figure 2). The Cys10 residue interacted with Ala52 as an atomic donor, but the Cys10 residue also acted as an atomic acceptor from Lys106 residue of MHC-II DRA1/DRB1 molecule. Residue Cys10 accepted atoms from residue Arg149 and donated atoms to Leu147 residue of HLA-DQA1*01:02/DQB1*06:01 which was facilitated by conventional hydrogen bond. Epitope 27-NVNDYEVVY-35 only interacted with domain A of MHC HLA-DQA1*01:02/DQB1*06:01 with three types of bonds. The types of bond were electrostatic, hydrogen and hydrophobic bond. Meanwhile, the 4-VLLVTICLA-12 epitope interacted with MHC HLA-DQA1*01:02/DQB1*06:01 both in domain A and domain B. Domain B of MHC HLA-DQA1*01:02/DQB1*06:01 more acted as an atomic donor than domain A of MHC HLA DQA1*01:02/DQB1*06:01. The energy was generated from the interaction between the 27-NVNDYEVVY-35 epitope with MHC HLA-DRA1/DRB1 and HLA-DQA1*01:02/DQB1*06:01 was lower than the interaction between the 4-VLLVTICLA-12 epitope with MHC HLA-DRA1/DRB1 and HLA-DQA1*01:02/DQB1*06:01 (Table 4).

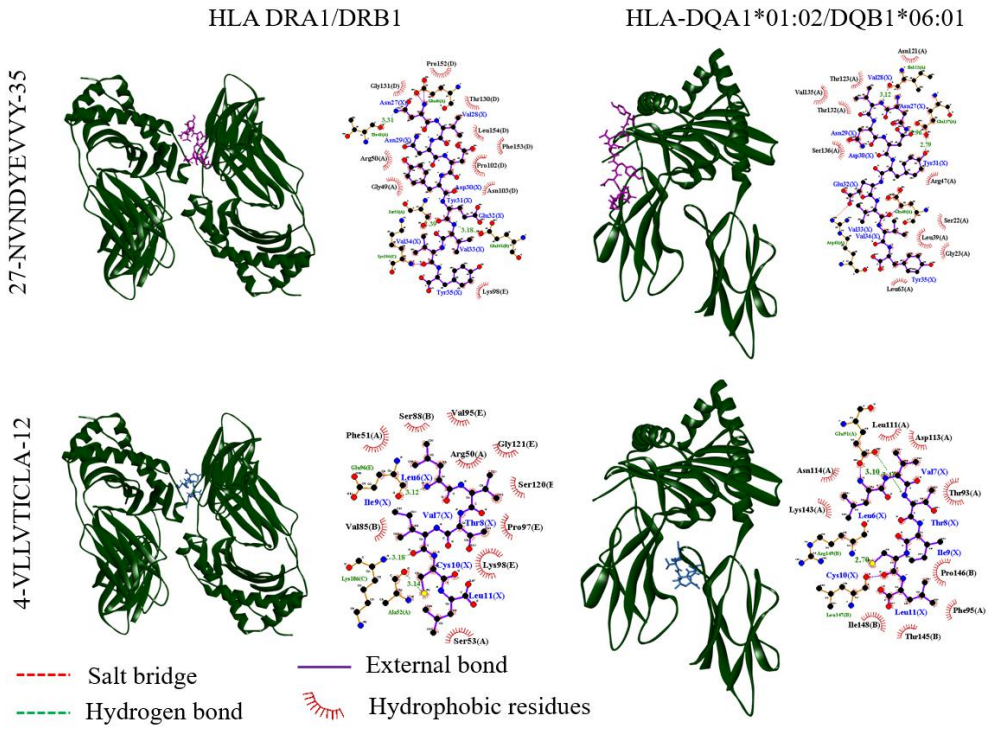

Figure 2. Interaction of epitope 4-VLLVTICLA-12 dan 27-NVNDYEVVY with MHC-II HLA-DRA1/DRB1 dan HLA-DQA1*01:02/DQB1*06:01. The color in 3D view denote as HLA (Green) 27-NVNDYEVVY epitope (Purple) and 4-VLLVTICLA-12 epitope (dark blue).

Table 3. Interaction MHC-I Alleles with 4-VLLVTICLA-12 dan 27-NVNDYEVVY-35 epitope

Interaction	Point Interaction	Category	Type	Binding energy (KJ/mol)
"GLKEGIPAL"-HLA-A*0201	**A:LYS243:NZ** - X:ALA8:O; **X:LEU2:N** - A:ASP30:OD1; **X:LYS3:NZ** - A:ASP29:OD2; **X:LYS3:NZ** - A:ASP30:OD1	Electrostatic	Attractive Charge	-463.7
	B:TYR63:HH - X:GLU4:O; **X:LYS3:HN** - A:ASP30:OD1	Hydrogen Bond	Conventional Hydrogen Bond	
	X:PRO7:CD - X:GLY5:O		Carbon Hydrogen Bond	
	X:LYS3:HZ1 - A:ASP30:OD2		Salt Bridge;Attractive Charge	
	A:ARG6 - X:LYS3	Hydrophobic	Alkyl	
	B:TYR26 - X:PRO7		Pi-Alkyl	
	X:GLY5:O - B:TYR63	Other	Pi-Lone Pair	
27-NVNDYEVVY-35-HLA-A*0201	**A:ARG65:NH2** - X:ASP30:OD2; **A:LYS66:NZ** - X:ASP30:OD1; **A:ARG97:NH1** - X:TYR35:OXT; **X:ASN27:N** - A:GLU55:OE1; **X:ASN27:N** - A:GLU58:OE2	Electrostatic	Attractive Charge	-426.4
	X:TYR35:OXT - A:TRP147		Pi-Anion	
	A:ARG65:HH11 - X:TYR31:O;	Hydrogen Bond	Conventional Hydrogen Bond	
	X:VAL33:CG1 - A:HIS70	Hydrophobic	Pi-Sigma	
	A:ALA69 - X:VAL33		Alkyl	
4-VLLVTICLA-12-HLA-A*0201	**X:LEU6:N** - A:ASP29:OD2; **X:LEU6:N** - A:ASP30:OD1	Electrostatic	Attractive Charge	-445.6
	B:LYS58:HN - X:CYS10:O; **B:LYS58:HN** - X:CYS10:SG; **B:TYR63:HH** - X:LEU11:OXT; **B:TYR63:HH** - X:THR8:O; **X:THR8:HN** - A:ASP30:OD1; **X:VAL7:HN** - A:ASP30:OD1	Hydrogen Bond	Conventional Hydrogen Bond	
	A:ARG6 - X:ILE9; **A:ALA211** - X:VAL7; **X:CYS10** - B:LYS58	Hydrophobic	Alkyl	
	A:TYR27 - X:ILE9; **B:TYR63** - X:LEU11		Pi-Alkyl	
27-NVNDYEVVY-35-HLA-B*15:02	**A:ARG21:NH2** - X:ASP30:OD1	Electrostatic	Attractive Charge	-414.4
	A:ARG21:HE - X:ASP30:O; **A:ASP37:HN** - X:GLU32:OE1; **A:ARG44:HN** - X:GLU32:OE1; **X:VAL28:HN** - B:ILE35:O; X:ASN29:HD22 - B:ASP34:OD1	Hydrogen Bond	Conventional Hydrogen Bond	

	A:PRO43:CA - X:GLU32:OE1		Carbon Hydrogen Bond	
	A:ARG21:NH2 - X:TYR31; **X:ASN27:N** - B:HIS51; **A:ASP37:OD2** - X:TYR31; **X:GLU32:OE1** - A:PHE36	Electrostatic	Pi-Cation	
	X:ASN27:CB - B:HIS51	Hydrophobic	Pi-Sigma	
	A:ALA40 - X:VAL34; **A:ALA41** - X:VAL34; **X:VAL28** - B:LEU54; **X:VAL28** - B:LEU64		Alkyl	
4-VLLVTICLA-12-HLA-B*15:02	**B:LYS58:NZ** - X:LEU11:OXT	Electrostatic	Attractive Charge	-411.1
	X:LEU11:O - A:TYR113		Pi-Anion	
	A:ARG6:HE - X:CYS10:O; **A:ARG6:HE** - X:LEU11:O **A:ARG6:HH22** - X:CYS10:O; **X:CYS10:SG** - A:ASP29:O;	Hydrogen Bond	Conventional Hydrogen Bond	
	X:VAL7:CA - A:ASP30:OD1		Carbon Hydrogen Bond	
	X:LEU6:HT2 - A:GLU212:OE2		Salt Bridge;Attractive Charge	
	A:ARG6 - X:CYS10; **A:PRO210** - X:VAL7; **A:ALA211** - X:LEU6; **A:ALA211** - X:VAL7; **B:LYS58** - X:ILE9	Hydrophobic	Alkyl	
	X:CYS10:SG - A:PHE8	Other	Pi-Sulfur	

Note : Bold as donor

Table 4. Interaction MHC-II with 27-NVNDYEVVY-35 and 4-VLLVTICLA-12 epitope

Interaction	Point Interaction	Category	Type	Binding energy (KJ/mol)
27-NVNDYEVVY-35-HLA-DRA1/DRB1	**C:LYS106:N** - X:TYR35:O	Electrostatic	Attractive Charge	-266.4 Kj
	A:SER53:HG - X:GLU32:O; **D:SER95:HG** - X:GLU32:OE1; **X:ASN27:HD21** - A:THR41:O; **X:VAL33:HN** - D:GLU101:OE1	Hydrogen Bond	Conventional Hydrogen Bond	
	D:PRO102:HA - X:ASP30:OD2; **D:PRO102:HD1** - X:TYR31:O; **X:GLU32:HA** - D:GLU101:OE1		Carbon Hydrogen Bond	
	C:LYS106 - X:VAL33; **D:PRO152** - X:VAL28	Hydrophobic	Alkyl	
4-VLLVTICLA-12-HLA-DRA1/DRB1	**C:LYS106:N** - X:LEU11:OXT; **E:LYS98:NZ** - X:LEU11:OXT; **X:LEU6:N** - E:GLU96:OE2	Electrostatic	Attractive Charge	-443.2 Kj
	C:LYS106:HT1 - X:ILE9:O; **C:LYS106:HT1** - X:CYS10:O; **C:LYS106:HT2** - X:ILE9:O; **X:LEU6:HT3** - E:GLU96:O; **X:CYS10:SG** - A:ALA52:O;	Hydrogen Bond	Conventional Hydrogen Bond	
	B:VAL345 - X:ILE9; **E:VAL95** - X:LEU6; **E:LYS98** - X:VAL7; **E:LYS98** - X:LEU11	Hydrophobic	Alkyl	
27-NVNDYEVVY-35-HLA-DQA1*01:02/DQB1*06:01	**A:LYS42:NZ** - X:TYR35	Electrostatic	Pi-Cation	-353.0
	X:ASN27:HD22 - A:GLU137:OE1; **X:VAL28:HN** - A:ILE122:O;	Hydrogen Bond	Conventional Hydrogen Bond	
	A:ARG41:HH22 - X:GLU32:OE1		Salt Bridge;Attractive Charge	
	X:VAL34 - A:LEU69	Hydrophobic	Alkyl	
4-VLLVTICLA-12-HLA-DQA1*01:02/DQB1*06:01	**X:LEU6:N** - A:ASP113:OD2	Electrostatic	Attractive Charge	-353.8
	B:ARG149:HN - X:CYS10:SG; **X:VAL7:HN** - A:GLU91:OE1; **X:THR8:HN** - A:GLU91:OE2; **X:CYS10:SG** - B:LEU147:O;	Hydrogen Bond	Conventional Hydrogen Bond	
	B:PRO146 - X:ILE9; **B:ILE148** - X:LEU11; **B:ARG149** - X:CYS10; **X:VAL7** - A:LEU111; **X:CYS10** - B:ILE148	Hydrophobic	Alkyl	
	A:PHE95 - X:LEU11		Pi-Alkyl	

Note : Bold as donor

Discussion

The 27-NVNDYEVVY-35 epitope easily interacted with MHC-I and MHC-II alleles, and interacted in α-helix and β-sheet structure of HLA-B*15:02 then tended to α-helix structure in MHC-II alleles. Each MHC-I and MHC-II alleles had different binding groove residues but had the same location. The β-sheet structure is the floor while the α-helix structure is the wall (Huang et al., 2015; Jones et al., 2006). The epitope of PLA_2 from Bungarus's venom easily interacted with MHC alleles and also interacted to the α-helix and β-sheet structures of MHC-I and MHC-II molecules (Kurniawan & Kurniasari, 2020; Muhammad Ashraf et al., 2014). Therefore, 27-NVNDYEVVY-35 can potent as candidate epitope for vaccine.

Not only that, Epitopes or peptides was made MHC complexes that must have a stronger bond with T cell receptors than MHC molecules (Piepenbrink et al., 2013). In addition, the recognition of T cells to the peptide-MHC complex (p-MHC) only occurred when there was a specification of the binding between the T cell receptor and the p-MHC complex or called MHC restriction phenomenon (Nielsen et al., 2003). Therefore, in further research was needed regarding the pattern of recognition of p-MHC from candidate epitope with T cell receptors.

T cell receptors recognized with p-MHC although it were varied (Nielsen et al., 2003). The MHC-1 recognized only with the 9 amino acids of peptide (Mohan & Unanue, 2012; Rubinstein et al., 2008). This was due to the closed binding nature of MHC-I. In contrast to MHC-II was had open binding properties. The MHC-II recognized with the 14-20 amino acids of peptides. Despite its open binding, only 9 amino acids have acted as registry peptides (Mohan & Unanue, 2012). Therefore, we can conclude that the 9-mer epitope predicted by the MHC-I molecule was possible to bound to the MHC-II molecule. Based on the docking simulation, the 27-NVNDYEVVY-35 epitope bound to MHC-I and MHC-II molecules with a suitable bonding location with low bond energy.

The bond energy of the candidate PLA_2 epitope with MHC molecules had a low bond energy. The low bond energy was also accorded with the number of hydrogen bonds. The good interaction epitope-MHC not only have low bond energy but also have more than three hydrogen bond (Jain et al., 2021; Kurniawan & Kurniasari, 2020). Hydrogen bonds were needed in the formation of p-MHC because it made p-MHC being stable (Li et al., 2014). The stability and hydrophilicity of the protein determined one of the properties that indicated the antigenicity of a protein (Rubinstein et al., 2008). Protein venom PLA_2 were hydrophilic and stable also had epitopes with high antigenicity (Alam & Ashraf, 2013; Kurniawan & Kurniasari, 2020). In addition to physico-chemical properties, the location of the epitope must be in the conserved domain and the protein must be endocytosed by the APC into the cell (León et al., 2011). The kistomin protein injected by *C. rhosostoma* in a mature form. Maturation of kistomin occurred in snake venom gland cells by deletion of signal peptides by peptidase enzymes and hydrolysis of snake venom prodomains before being transported to the lumen of gland cells (Moura-da-Silva et al., 2016). Thus, only the metalloproteinase domain was endocytosed by Antigen-Presenting Cell (APC) and both candidates epitopes the 4-VLLVTICLA-12 and the 27-NVNDYEVVY-35 were not found as a result of intracellular or extracellular degradation because the amino acid sequence was in the signal peptide domain and pro-domain.

Degradation or denaturation of antigen served to destroy or cut antigen proteins in order to form p-MHC complexes (Piepenbrink et al., 2013). MHC molecules in humans were called Human Leukocyte Antigen (HLA) whose it were polymorphic (Choo, 2007). This polymorphic trait was very useful in evolution and conservation (Sommer, 2005). The variation was associated with the interaction between peptide and MHC molecules in p-MHC formation and recognition by T cell receptors (Mohan & Unanue, 2012; Nielsen et al., 2003). However, one epitope can be recognized by several different MHC molecules (Alam & Ashraf, 2013; Kurniawan & Kurniasari, 2020; Muhammad Ashraf et al., 2014). Therefore, the selection of HLA for prediction is very important.

In conclusion, the conserved and highly immunogenic epitope are 4-VLLVTICLA-12 and 27-NVNDYEVVY-35, which the region of epitopes are in signal peptide and pro-domain. Epitope 4-VLLVTICLA-12 does not induce an immune response whereas epitope 27-NVNDYEVVY-35 can induce an immune response in human with HLA-A*02:01. In the future, other alleles can be used to predict the epitope and can be focused metalloproteinase domain of kistomin.

Acknowledgement

This study was supported by UB Professorship 2020-2021 to Fatchiyah and PDUPT National Research grant 2020-2021 to Nia Kurniawan. We thank to members of the Research Center of SMONAGENES UB and working group NK research who have provided support and advice. We thank also to Dewi Ratih Tirto Sari and Hagar Ali Marzouk for review translated.

References

Ahkam AH., Hermanto FE., Alamsyah A., Aliyyah IH., and Fatchiyah F., 2020. Virtual Prediction of Antiviral Potential of Ginger (*Zingiber Officinale*) Bioactive Compounds Against Spike and MPro of SARS-CoV2 Protein. *Berkala Penelitian Hayati* 25(2):52–57.

Alam MJ., and Ashraf KUM., 2013. Prediction of an Epitope-based Computational Vaccine Strategy for Gaining Concurrent Immunization Against the Venom Proteins of Australian Box Jellyfish. *Toxicology International* 20(3):235–253.

Andreatta M., and Nielsen M., 2016. Gapped Sequence Alignment Using Artificial Neural Networks: Application to the MHC Class I System. *Bioinformatics (Oxford England)* 32(4):511–517.

Bermúdez-Méndez E., Fuglsang-Madsen A., Føns S., Lomonte B., Gutiérrez JM., and Laustsen AH., 2018. Innovative Immunization Strategies for Antivenom Development. *Toxins* 10(452):1-37.

Bui HH., Sidney J., Li W., Fusseder N., and Sette A., 2007. Development of an Epitope Conservancy Analysis Tool to Facilitate The Design of Epitope-Based Diagnostics And Vaccines. *BMC Bioinformatics* 8:361.

Choo S., 2007. The HLA System: Genetics Immunology Clinical Testing and Clinical Implications. *Yonsei Medical Journal* 48(1):11-23.

Das I. 2015. A Field Guide to the Reptiles of South-East Asia. London: Bloomsbury Publishing Plc.

Fatchiyah F., Raharjo SJ., and Dewi FRP., 2015. Virtual Selectivity Peptides OF CSN1S2 Protein of Local Goat Ethawah Breeds Milk Modulate Biological Mechanism of Calmodulin. *International Journal of Pharma and Bio Sciences* 6(2):707–718.

Gutiérrez JM., Escalante T., Rucavado A., Herrera C., and Fox JW., 2016. A Comprehensive View of the Structural and Functional Alterations of Extracellular Matrix by Snake Venom Metalloproteinases (SVMPs): Novel Perspectives on the Pathophysiology of Envenoming. *Toxins* 8(304):77-97.

Huang R., Yin J., Chen Y., Deng F., Chen J., Gao X., Liu Z., Yu X., and Zheng J., 2015. The Amino Acid Variation within The Binding Pocket 7 And 9 Of HLA-DRB1 Molecules are Associated with Primary Sjögren's Syndrome. *Journal of Autoimmunity* 57:53–59.

Jain R., Jain A., and Verma SK., 2021. Prediction of Epitope Based Peptides for Vaccine Development from Complete Proteome of Novel Corona Virus (SARS-COV-2) Using Immunoinformatics. *International Journal of Peptide Research and Therapeutics* 27:1729–1740

Jones EY., Fugger L., Strominger JL., and Siebold C., 2006. MHC Class II Proteins and Disease: A Structural Perspective. *Nature Reviews Immunology* 6(4):271–282.

Kasturiratne A., Wickremasinghe AR., de Silva N., Gunawardena NK., Pathmeswaran A., Premaratna R., Savioli L., Lalloo DG., and de Silva HJ., 2008. The Global Burden of Snakebite: A Literature Analysis and Modelling Based on Regional Estimates of Envenoming and Deaths. *PLoS Medicine* 5(11) :1591-1604.

Khan MA., Hossain MU., Rakib-Uz-Zaman SM., and Morshed MN., 2015. Epitope-Based Peptide Vaccine Design and Target Site Depiction Against Ebola Viruses: An Immunoinformatics Study. *Scandinavian Journal of Immunology* 82(1):25–34.

Kurniawan N., and Kurniasari CA., 2020. In Silico Prediction of Malayan Krait (*Bungarus candidus*) PLA_2 Epitope. *Systematic Reviews in Pharmacy* 11(10):537-548.

León G., Sánchez L., Hernández A., Villalta M., Herrera M., Segura A., Estrada R., and Gutiérrez JM., 2011. Immune Response Towards Snake Venoms. *Inflammation & Allergy Drug Targets* 10(5):381–398.

Li W., Joshi M., Singhania S., Ramsey K., and Murthy A., 2014. Peptide Vaccine: Progress and Challenges. *Vaccines* 2(3):515–536.

Lundegaard C., Lamberth K., Harndahl M., Buus S., Lund O., and Nielsen M., 2008. NetMHC-3.0: Accurate Web Accessible Predictions of Human Mouse and Monkey MHC class I Affinities for Peptides of Length 8-11. *Nucleic Acids Research* 36(Web Server issue):W509-W512.

Mohan JF., and Unanue ER., 2012. Unconventional recognition of peptides by T cells and the implications for autoimmunity. *Nature Reviews. Immunology* 12(10):721–728.

Moura-da-Silva AM., Almeida MT., Portes-Junior JA., Nicolau CA., Gomes-Neto F., and Valente RH., 2016. Processing of Snake Venom Metalloproteinases: Generation of Toxin Diversity and Enzyme Inactivation. *Toxins* 8(183):1-15.

Muhammad Ashraf KU., Barua P., Saha A., Mahammad N., Ferdoush J., Das D., Hussain H., and Alam J., 2014. An Immunoinformatics Approach Toward Epitope-Based Vaccine Design Through Computational Tools from *Bungarus caeruleus*'s Neurotoxin. *Journal of Young Pharmacists 6*(2):35–43.

Nielsen M., Lundegaard C., Worning P., Lauemøller SL., Lamberth K., Buus S., Brunak S., and Lund O., 2003. Reliable Prediction of T-Cell Epitopes Using Neural Networks with Novel Sequence Representations. *Protein Science* 12(5):1007–1017.

Olaoba OT., Santos PK., dos Selistre-de-Araujo HS., and Souza DHFde., 2020. Snake Venom Metalloproteinases (SVMPs): A Structure-Function Update. *Toxicon* X7 (100052):1-15.

Parvizpour S., Pourseif MM., Razmara J., Rafi MA., and Omidi Y., 2020. Epitope-Based Vaccine Design: A Comprehensive Overview of Bioinformatics Approaches. *Drug Discovery Today* 25(6):1034–1042.

Piepenbrink KH., Blevins SJ., Scott DR., and Baker BM., 2013. The Basis for Limited Specificity and MHC Restriction in A T Cell Receptor Interface. *Nature Communications* 4(1948):1-21.

Rubinstein ND., Mayrose I., Halperin D., Yekutieli D., Gershoni JM., and Pupko T., 2008. Computational Characterization of B-cell Epitopes. *Molecular Immunology* 45(12):3477–3489.

Sette A., and Fikes J., 2003. Epitope-Based Vaccines: An Update on Epitope Identification Vaccine Design and Delivery. *Current Opinion in Immunology* 15(4):461–470.

Sommer S., 2005. The importance of immune gene variability (MHC) in evolutionary ecology and conservation. *Frontiers in Zoology* 2(16):1-18.

Tang ELH., Tan CH., Fung SY., and Tan NH., 2016. Venomics of *Calloselasma rhodostoma* the Malayan pit viper: A Complex Toxin Arsenal Unraveled. *Journal of Proteomics* 148:44–56.

Tang ELH., Tan NH., Fung SY., and Tan CH., 2019. Comparative Proteomes Immunoreactivities and Neutralization of Procoagulant Activities of *Calloselasma rhodostoma* (Malayan Pit Viper) Venoms from Four Regions in Southeast Asia. *Toxicon: Official Journal of the International Society on Toxinology* 169:91–102.

Tapiory AA., Pertiwi KO., Fadilla K., Reyhanditya D., and Fatchiyah F., 2020. *In-Silico* Analysis of Methoxyl Pectin Compounds from Banana Peels as HMG-CoA Reductase Inhibitor Complexes. *JSMARTech: Journal of Smart Bioprospecting and Technology* 1(2):046–050.

World Health Organization. 2010. WHO Guidelines for The Production Control and Regulation of Snake Antivenom Immunoglobulins. Geneva:WHO Press.